Garlic-derived organosulfides induce cytotoxicity, apoptosis, cell cycle arrest and oxidative stress in human colon carcinoma cell lines[*]

J. JAKUBÍKOVÁ, J. SEDLÁK

Laboratory of Tumor Immunology, e-mail: exonjana@savba.sk, Cancer Research Institute, 833 91 Bratislava, Slovak Republic

Organosulfur compounds (OSC) from garlic, especially allicin (ALI), diallyl sulfide (DAS), diallyl disulfide (DADS), and diallyl trisulfide (DATS) are recognized as a group of potential chemopreventive agents. In this study, we examined the effects of OSC on human Caco-2 and HT-29 colon carcinoma cell lines. Apoptosis induction (Annexin-V-FITC/PI, fluorescein diacetate/PI, sub-G1 fraction), modulation of DNA cell cycle (G2/M arrest, phospho-H3 mitotic marker), transmembrane mitochondrial potential (JC-1) and intracellular GSH amount (monochlorobimane assay) were measured by flow cytometry and fluorimetry. Our results showed that order of OSC-induced cell death in Caco-2 and HT-29 cells increased in the range as follows: ALI<DAS=DADS<DATS and ALI=DAS<DADS<DATS, respectively. Both cell lines used are relatively resistant to OSC induced cytotoxicity, because compound concentrations required to obtain significant effect are in high micromolar range. ALI was less toxic than equimolar doses of other OSC tested with the exception of GSH modulation and G2/M arrest in Caco-2 cells. DADS-treated HT-29 cells and both DATS-treated cell lines exhibit inverse correlation between p-H3 positivity and compound concentration due to higher apoptotic rate. These results show the correlation of sulfur atoms number in OSC with their capacity in apoptosis induction and support the role of redox-sensitive "sulfhydryl switches" in maintaining intracellular redox milieu.

Key words: organosulfur compounds, apoptosis, mitotic arrest, redox, human colon cancer cell lines

Garlic and garlic supplements, most likely for their high content of the water- and lipid-soluble organosulfur compounds (OSC) [1] have been considered to be one of the best disease-preventive food [2–5]. Alliin, a product of hydrolyzed gand oxidized primary sulfur-containing compounds γ-glutamyl-S-alk(en)yl-L-cysteines, is the odorless precursor of OSC. The enzyme alliinase is released by processing of garlic bulb and acts upon alliin to produce odoriferous thiosulfinates such as allicin. Allicin and other thiosulfinates decompose to oil-soluble OSC, including diallyl sulfide (DAS), diallyl disulfide (DADS) and diallyl trisulfide (DATS) (Fig. 1). Numerous studies provide evidence that increased consumption of garlic is associated with a marked reduction in cancer risk. These studies revealed that consumption of garlic or its constituents by experimental animals reduced
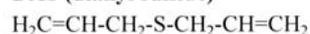
Abbreviations: OSC – organosulfur compounds; ALI – allicin; DAS – diallyl sulfid; DADS – diallyl disulfide; DATS – diallyl trisulfide; MAPK – mitogen-activated protein kinase; JNK – c-Jun N-terminal kinase; ERK1/2 – extracellular signal-regulated kinases 1 and 2; ROS – reactive oxygen species; JC-1 – 5,5',6,6'-tetrachloro-1,1',3,3'-tetraethylbenzimidazolyl carbocyanine iodide, FDA – fluorescein diacetate; PI – propidium iodide; BSO – D,L-buthionine (S,R)-sulfoximine; MTT – 3-[4,5-dimethylthiazol-2-yl]-2,5-diphenyl tetrazolium bromide; MCB – monochlorobimane; GSH – glutathione, MMP – mitochondrial membrane potential

ALI (allicin)
$H_2C=CH-CH_2-SO-CH_2-CH=CH_2$
DAS (diallyl sulfide)
$H_2C=CH-CH_2-S-CH_2-CH=CH_2$
DADS (diallyl disulfide)
$H_2C=CH-CH_2-S-S-CH_2-CH=CH_2$
DATS (diallyl trisulfide)
$H_2C=CH-CH_2-S-S-S-CH_2-CH=CH_2$
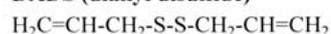
Figure 1. Chemical structures of OSC used in this study.

chemically induced esophageal, skin, pulmonary, fore-stomach, colon, mammary, and lung tumors [6–9].

Various pathways have been suggested for the anti-carcinogenic activity of OSC, including modulation of xeno-biotic-metabolizing enzyme activities [10], inhibition of DNA adduct formation [11], modulation of signal trans-duction pathways [12], inhibition of proliferation [13], and induction of apoptosis [14]. Although the role(s) and/or mechanism(s) of OSC as anticancer agents remain unclear, there is an increasing evidence of possible molecular targets involved such as ERK1/2 [15], p38 [16], and JNK MAPK [17], Nrf2 nuclear translocation, and enhanced phase II de-toxifying enzyme gene expression [18]. Recently, complex pattern of molecular changes in the G2/M arrest [19], tubulin oxidation [20], increase of p21$^{Waf1/Cip1}$ expression and histone deacetylase (HDAC) inhibition [21] were found.

The aim of our study was to assess the effect of potential chemopreventive activities of OSC on the vital cellular pathways such as mitochondrial membrane potential mainte-nance, intracellular redox regulation, and cell division in hu-man colon carcinoma cell lines. The results show that OSC tested induce G2/M arrest, disrupt mitochondrial membrane potential and modulate intracellular GSH amount, and exert cytotoxic effect through induction of apoptosis.

Material and methods

Reagents. Allicin (ALI), diallyl sulfide (DAS), diallyl disulfide (DADS) and diallyl trisulfide (DATS) were pur-chased from LKT Laboratories (St. Paul, MN). Polyclonal an-tibodies against phospho-histone H3 (p-H3) and FITC-con-jugated anti-rabbit IgG were purchased from Biomol Research Laboratories (Hamburg, Germany) and Sigma (Dorset, UK), respectively. The Annexin V-FITC apoptosis detection kit was from BD Biosciences Pharmingen. Fluorescein diacetate (FDA), dimethyl sulfoxide (DMSO), RNA-se A, propidium iodide (PI), $_{D,L}$-buthionine (S,R)-sulf-oximine (BSO) and 3-[4,5-dimethylthiazol-2-yl]-2,5-di-phenyl tetrazolium bromide (MTT) were obtained from Sigma (Dorset, UK). JC-1 (5,5',6,6'-tetrachloro-1,1',3,3'-te-traethylbenzimidazolyl carbocyanine iodide) and MCB (monochlorobimane) were purchased from Molecular Probes (Eugene, OR).

Cell culture and treatment with OSC. The human colon adenocarcinoma cell line Caco-2 and HT-29 were obtained from the European Collection of Cell Culture (Wiltshire, UK). Stock cells were cultured in RPMI 1640 medium sup-plemented with 10% fetal calf serum, 100 µg/ml penicillin and 50 µg/ml streptomycin in humidified air atmosphere with 5% CO_2 at 37 °C. The cultures were maintained for 4–5 days prior to experimental treatment. The cells were treated on ∅ 60 mm dishes when cultures achieved about 50–60% of confluence. Stock solutions of OSC were originally dis-solved in DMSO. Cells were exposed to various concentra-tions of OSC for varying lengths of time as indicated and an

equal volume of DMSO (final concentration <0.1%) was added to the control cells. The floating cells were collected by centrifugation at 700 x g for 3 min, whereas adherent cells were trypsinized and collected by centrifugation at 700 x g for 3 min. Pooled cells were washed twice with cold PBS.

Cell survival assay. The viability of cultured cells was de-termined by assaying for the reduction of MTT to formazan. The cells (5 x 10^3 per well in 200 µl of medium) were seeded in a 96-well culture plate, left to adhere to the plastic and grown to reach 50–60% confluence before they were ex-posed to OSC. In each experiment, the dose of OSC was tested in quadruplicate, and the cytotoxicity curve was con-structed from at least six (50, 100, 200, 500, 1000 and 2000 µM) different concentrations of OSC. After 24, 48 and 72 h, the cells were incubated with 50 µl of MTT (1 mg/ml) and left in the dark at 37 °C for an additional 4 h. Thereafter, medium was removed, the formazan crystals were dissolved in 200 µl of DMSO, and the absorbance was measured at 540 and 690 nm in a Multisoft plate reader (Labsystems Oy, Fin-land).

Cytofluorimetric analysis of mitochondrial potential. Vari-ations of MMP in OSC-treated cells were studied using JC-1 fluorescent probe. Approximately 5 x 10^5 cells were incu-bated in 400 µl of PBS/0.2% BSA containing 4 µM of JC-1 (from a 7.7 mM stock in DMSO) for 30 min at 37 °C. After 30 min incubation in the dark at 37 °C, the cells were ana-lysed using a Coulter Epics Altra flow cytometer.

Annexin V-FITC staining. Apoptotic cells were quantified using the Annexin V-FITC Apoptosis detection kit according to the manufacturer's instructions. Approximately 5 x 10^5 cells were resuspended in 100 µl of manufacturer-supplied 1 x binding buffer, and mixed with 5 µl of Annexin V-FITC and 5 µl of PI. After 15 min incubation in the dark at room temperature, the cells were analyzed using a Coulter Epics Altra flow cytometer.

Fluorescein diacetate (FDA)/PI staining. Approximately 5 x 10^5 cells were resuspended in 400 µl of PBS/0.2% BSA containing 10 nM of FDA (from a 5 mM stock in DMSO) for 30 min at room temperature. Then cells were cooled and 4 µl of PI (1 mg/ml) was added. Finally, after 15 min the stained cells were analyzed using a Coulter Epics Altra flow cyto-meter.

Cell cycle analysis. This determination was based on the measurement of the DNA content of nuclei labeled with PI. For flow cytometry analyses of DNA cell cycle profile, ap-proximately 5 x 10^5 cells were resuspended in 0.05% Triton X-100 and 15 µl of RNA-se A (10 mg/ml) for 20 min at 37 °C. After cooling on ice for at least 10 min, PI (50 µg/ml) was added. Finally, after 15 min the stained cells were ana-lyzed using a Coulter Epics Altra flow cytometer.

Detection of phospho-histone H3 activation. For flow cytometric analysis of phospho-histone H3 expression, ap-proximately 1 x 10^6 cells were fixed in 1% methanol-free paraformaldehyde in PBS at 0 °C for 3 min, washed in PBS/0.2% BSA and then resuspended in 70% ethanol for at

least 2 h at -20 °C. The cells were then washed twice in 1% solution of BSA in PBS to suppress non-specific antibody binding. Then the cell pellet was suspended in 100 µl of 1% BSA containing 1:200 diluted anti-phosphohistone H3 polyclonal antibody. Cells were incubated for 1 h at room temperature, washed twice with PBS/1% BSA, and resuspended in 100 µl of 1:60 diluted FITC-conjugated anti-rabbit immunoglobulin for 30 min at room temperature in the dark. After double washing in PBS, cells were counterstained with 5 µg/ml of PI dissolved in PBS, for 15 min at 4 °C. Cellular fluorescence was measured using a Coulter Epics Altra flow cytometer.

Monochlorobimane (MCB) assay. The cells (5×10^3 per well in 200 µl of medium) were seeded in a 96-black well clear bottom culture plate and left to adhere and reach 50–60% confluence before being exposed to OSC. The cells were exposed to test compounds for 3, 6 and 24 h and each dose of OSC was tested in quadruplicate. At the end of incubation period, the cells monolayers were washed twice with PBS and incubated with monochlorobimane (MCB; 40 µM) in the dark for 20 min at room temperature. After washing twice with PBS, plate was measured at 405/510 nm (excitation/emission) using POLARstar fluorimeter (BMG Labtech, Offenburg, Germany).

Flow cytometry measurements and data analysis. Coulter Epics Altra flow cytometer was equipped with 488 nm excitation laser and fluorescence emissions were measured using bandpass filter set 525, 575, 610, and 675 nm. Forward/side light scatter characteristic was used to exclude the cell debris from the analysis. For each analysis, 1×10^4 cells were acquired for analysis. Data were analyzed with WinMDI version 2.7 software (J. Trotter, Scripps Research Institute, La Jolla, CA). The cell cycle calculations were performed with MULTI-CYCLE Software (Phoenix Flow System).

Results

Cytotoxic effect of garlic-derived organosulfides. The effects of the OSC analogues on cell survival of colon adenocarcinoma cell lines Caco-2 and HT-29 were determined by MTT assay. The cell viability of both cell lines was not changed after 24 h treatement with OSC analogues with the exception of the highest concentrations of DATS (data not shown). Nearly 30% reduction of cell viability was achieved after 48 h treatment. Based on these findings and of others [18] we have selected 3 concentrations of OSC for further study.

To confirm the cytotoxic effect of OSC analogues, cell damage was estimated by the loss of MMP values. Measurement of JC-1 monomers aggregation was used to delineate OSC-induced MMP alterations. The representative dot plots are shown in Figure 2A, where JC-1 aggregates accumulate in control cells and display high orange signal (top right quadrant). Production of JC-1 monomers directly correlates to changes of MMP and its breakdown in dying cells results

in increase of green fluorescence (68% of cells in bottom right quadrant). Caco-2 cells exposed to DATS had a significant decrease of MMP in a dose-dependent manner (53–68% of cells) while cells treated with DADS, ALI and DAS showed only slight change of mitochondrial potential (Fig. 2B) in comparison to control (DMSO treated) cells. As shown in Figure 2C, about 97–93% of the HT-29 cells were
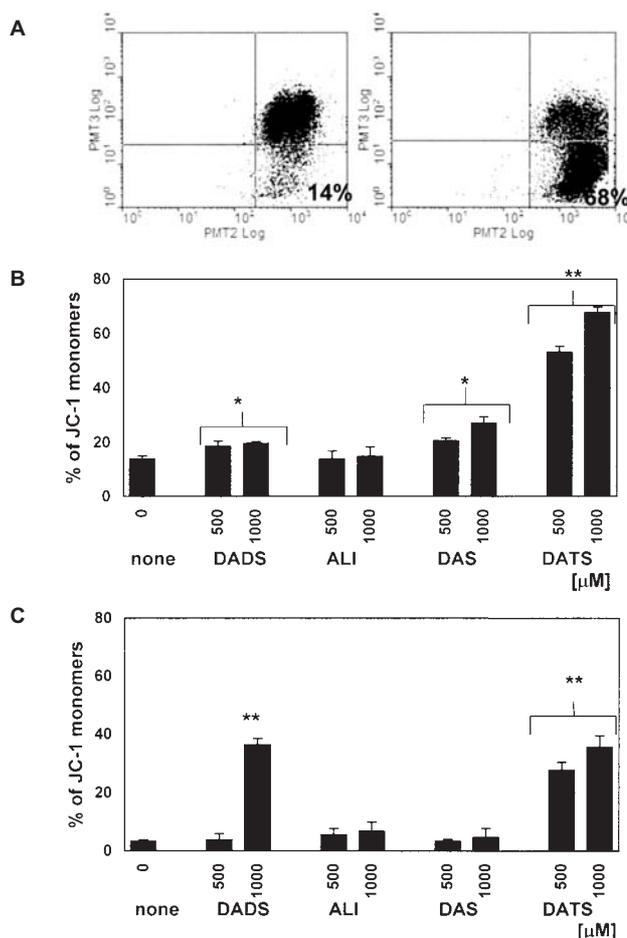

Figure 2. Effect of OSC on induction of mitochondrial membrane depolarization in Caco-2 and HT-29 cells. (A) The Caco-2 control cells (left dot blot) and cells treated with 1000 µM DATS (right dot plot) for 48 h and stained with the mitochondria selective JC-1 dye. Cells with polarized mitochondrial membranes emit green-orange fluorescence (top right quadrant). The number in the bottom right quadrant of each dot plot represents the percentage of cells that emit only green fluorescence attributable to depolarized mitochondrial membranes. (B) Effect of OSC on induction of mitochondrial membranes depolarization in Caco-2 and (C) HT-29 cells treated for 48 h. Changes of the JC-1 monomers production as a function of the ITCs concentration are shown. The cells were exposed to either DMSO (control) cells or two concentrations (500 µM and 1000 µM) of OSC (DADS, ALI, DAS, and DATS), stained with JC-1 dye and analyzed using a coulter Epics Altra flow cytometer with photomultipliers FL1, FL2, ratio FL2/FL1 required for fluorochrome JC-1. The data presented are from the three independent experiments; and the results are means ± SE. Significant difference from controls, *p<0.05; **p<0.01.

viable with normal polarized mitochondrial membranes after 48 h exposure to DAS and ALI, whereas 36% cells have disrupted MMP after DADS and DATS treatment at the highest concentrations.

Apoptosis induction by OSC. Next, we addressed the question whether growth suppressive effect of the OSC analogues correlates with apoptosis induction, which is a widely accepted mechanism for antiproliferative activity of many therapeutic agents [22]. Apoptosis-inducing effects of OSC analogues were assessed by Annexin V/PI assay. Transmembrane externalization of phosphatidylserine is a recognized early event of apoptosis, detection of which by flow cytometry-based Annexin V staining is widely used for early apoptotic cells identification. Propidium iodide is a standard flow cytometric viability probe, which is used in combination with Annexin V to distinguish between early apoptotic (Annexin V^+/PI^-) and late apoptotic/necrotic cells (Annexin V^+/PI^+, double positive). As shown in Figure 3A and 3B, flow cytometric analyses of Annexin V staining revealed increase of both early apoptotic and late apoptotic/necrotic cells amounts according to OSC concentration. The percentage of Annexin V^+/PI^- cells was increased in the range of 2.1

to 4.1-fold and Annexin V^+/PI^+ in the range of 2.6 to 3.3-fold in DATS-treated Caco-2 cells (Fig. 3A). In addition, the significant increase of late apoptotic/necrotic populations in DADS and DAS-treated Caco-2 cells was observed. Similar to Caco-2 cells, the 48 h exposure of HT-29 cells to DATS resulted in significant increase of Annexin V^+/PI^- and Annexin V^+/PI^+ cells in comparison with mDMSO-treated control (Fig. 3B). The highest concentration (1000 M) of the most effective DATS increased the percentage of Annexin V^+/PI^- and Annexin V^+/PI^+ cells to 19% and 26%, respectively. Contrary to DATS-treated cells, induction of apoptosis and necrosis was not significantly increased upon a 48 h exposure of HT-29 cells to DADS, ALI or DAS.

To confirm the apoptotic process, FDA/PI staining, another method for monitoring apoptosis was used [23]. Viable cells take up the fluorogen FDA, activate it by non-specific esterases and retain the free fluorescein in their cytoplasm. Apoptotic and dead cells show reduced turnover or no uptake of FDA and counterstaining with PI identifies dead cells. Figures 3C and 3D depict the percentage of apoptotic (FDA$^-$/PI$^-$) and necrotic (FDA$^-$/PI$^+$) cells as a function of OSC concentration. In comparison with Annexin V/PI staining, exposure
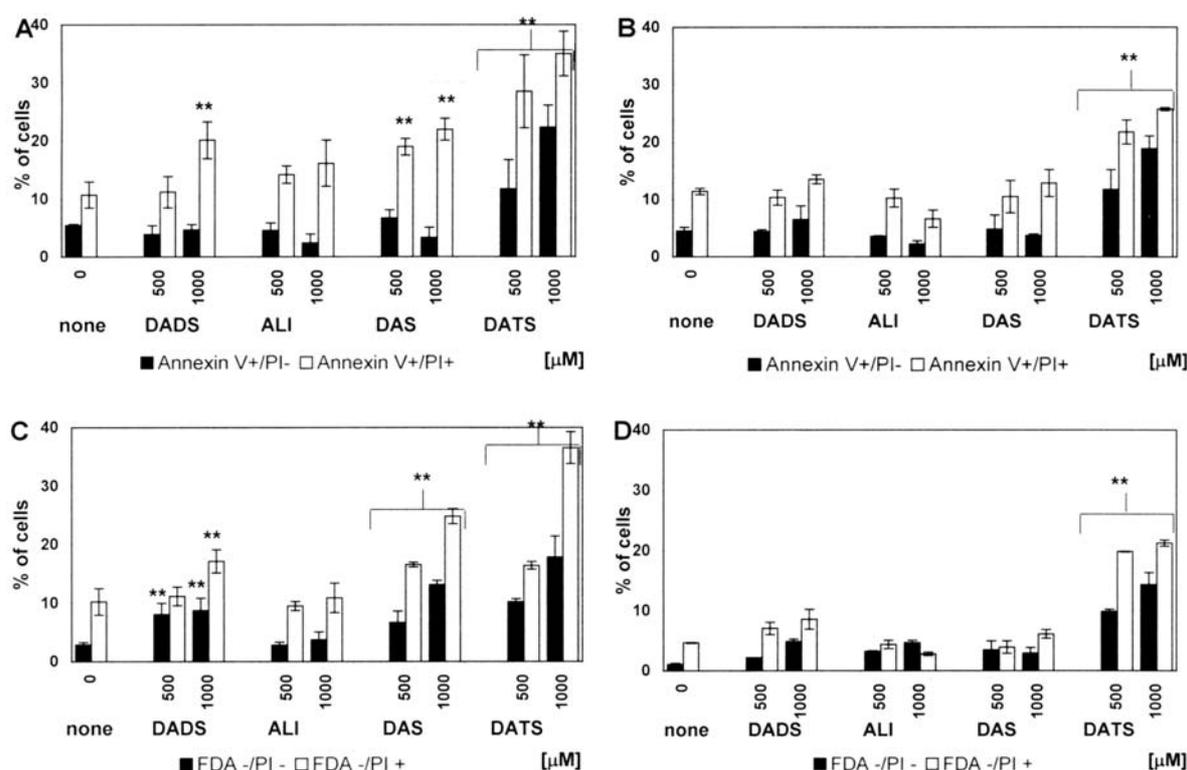

Figure 3. Effect of OSC treatment on apoptosis and necrosis induction in Caco-2 and HT-29 cells. (A) Percentage of apoptotic (Annexin V^+/PI^-) and late apoptotic/necrotic (Annexin V^+/PI^+) cells was shown. Exposure to either DMSO (control) cells or different concentrations of OSC (DADS, ALI, DAS, and DATS) treated Caco-2 cells and (B) HT-29 cells for 48 h. (C) Percentage of apoptotic (FDA$^-$/PI$^-$) and late apoptotic/necrotic (FDA$^-$/PI$^+$) cells were shown. Exposure to either DMSO (control) cells or different concentrations (500 μM and 1000 μM) of OSC (DADS, ALI, DAS, and DATS) treated Caco-2 cells and (D) HT-29 cells for 48 h. The cells were analyzed using a coulter Epics Altra flow cytometer with photomultipliers FL1 required for fluorochrome Annexin V-FITC and FDA and FL2 for PI. The data presented is from the three independent experiments; and the results are means ± SE. Significant difference from the controls, **p<0.01.

of both cell lines to OSC resulted in a similar percentage increase of apoptotic and necrotic cells in a dose-dependent manner with the exception of higher necrotic fraction in Caco-2 cells treated with DADS and DAS.

Flow cytometric analysis of cells with sub-G1 DNA content following staining with propidium iodide is a widely accepted technique for apoptosis detection. Exposure of Caco-2 and HT-29 cells to DATS and DADS resulted in a statistically significant increase in the fraction of sub-G1 cells at both concentrations compared to control (Fig. 4). On the other hand, DAS or ALI showed only very slight increase and did not affect significantly the increase of sub-G1 cell subpopulation. Overall, these results indicated that antiproliferative activity of DATS against HT-29 and Caco-2 cells correlated with their ability to induce apoptotic cell death.

Mitotic block by OSC. The effect of OSC on cell proliferation was evaluated by measuring the distribution of cells in different phases of the cell cycle. Flow cytometric cell cycle analysis showed an accumulation of Caco-2 cells in G2/M cell cycle phase after treatment with DATS and ALI for 24 h (Fig. 5A). A tremendous increase of G2/M cells at the expense of G0/G1 cells decrease was found in DATS and DADS treated HT-29 cells. While DADS showed concentration-dependent increase of G2/M, in the case of DATS an inverse correlation between G2/M accumulation and DATS concentration was observed (Fig. 5B).

To assess the proportion of mitotic cells within G2/M cells, the two-color flow cytometry measurement of phospho-histone H3 (p-H3) positive cells in G2/M population was performed. The representative histograms of p-H3 staining on gated G2/M populations are shown in Figure 6A. Regardless the significant ALI-induced G2/M accumulation (Fig. 5A) no p-H3 positivity in ALI-treated Caco-2 cells was observed (Fig. 6B). In contrast, ALI-treated HT-29 cell induced p-H3 positive mitotic cells more readily. DADS-treated HT-29 cells and both DATS-treated cell lines exhibit inverse corre-

lation between p-H3 positivity and compound concentration. Taking into account that DATS was the most potent apoptosis inducer (Fig. 3 and 4) we can speculate, that decreased p-H3 fraction of G2/M cells is due to higher apoptotic rate proportional to DATS concentration used.

Depletion of reduced glutathione (GSH) by OSC. To determine whether cytotoxicity of OSC in colon cancer cell lines is associated with oxidative stress, we measured the levels of reduced intracellular GSH in cells exposed to OSC (Fig. 7). MCB is versatile, membrane permeable nonfluorescent probe that binds irreversible to sulfhydryl groups with high reactivity to reduced GSH yielding a fluorescent product. Pre-treatment of cells with 500 µM BSO for 24 h was used as a control of decreased intracellular GSH level. This treatment reduced GSH amount to 25% and 70% of untreated control Caco-2 and HT-29 cells, respectively (data not shown). The most profound GSH decrease was achieved after exposure of Caco-2 and HT-29 cells to DATS in the concentration and time-dependent manner (Fig. 7A and 7B). Exposure of Caco-2 cells to DAS decreased the level of reduced GSH at 3 h and 6 h of treatment followed by increase of GSH amount to the level of control cells at 24 h. ALI-treatment of Caco-2 cells decreased GSH to level sustained at all time points measured, while both concentrations of DADS did not deplete the amount of reduced GSH. No significant change of intracellular GSH was found in ALI- and DAS-treated HT-29 cells (Fig. 7B). Treatment of HT-29 cells with DADS at both
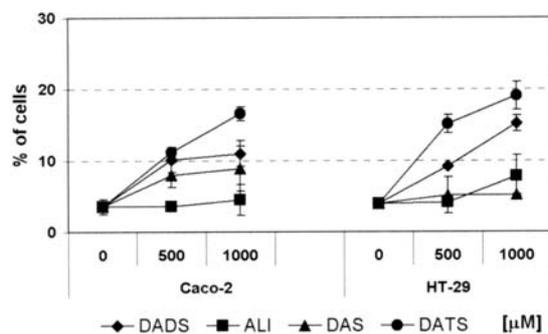

Figure 4. Effect of OSC on sub-G1 phase induction in Caco-2 and HT-29 cells. The Caco-2 and HT-29 cells were exposed to DMSO (control) or two concentrations (500 µ and 1000 µM) of OSC (DADS, ALI, DAS, and DATS) for 48 h. The cells were collected; detergent permeabilized and stained with 50 µg/ml concentration of PI in the presence of RNA-se A. Three independent experiments were performed and mean ± SE are presented.
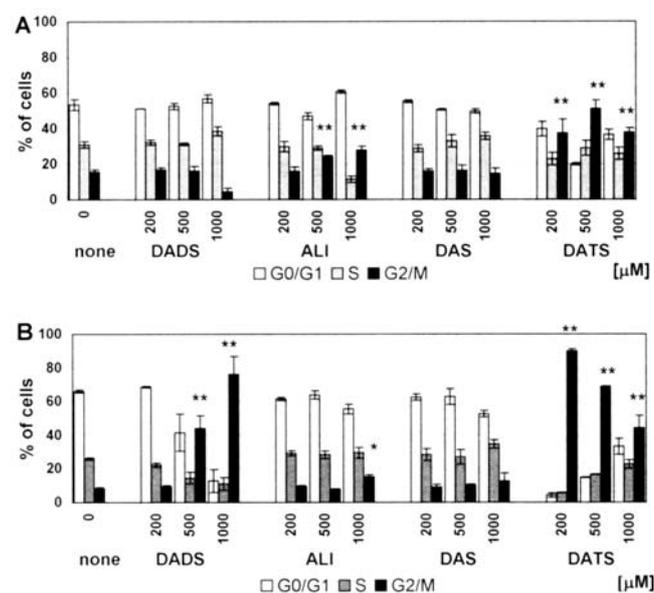
Figure 5. The effect of OSC on cell cycle in Caco-2 and HT-29 cells. (A) The Caco-2 and (B) HT-29 cells were exposed to DMSO (control) or different concentrations (200 µM, 500 µM, and 1000 µM) of OSC (DADS, ALI, DAS, and DATS) for 24 h. The distribution of cells in G0/G1, S and G2/M phase was analyzed by Multi-cycle software. Three independent experiments were performed and mean ± SE are presented. Significant difference from controls, *p<0.05; **p<0.01.

concentrations decreased the level of reduced GSH at 3 h, but after 6 h and 24 h exposure to DADS the amount of reduced GSH was comparable to control untreated cells. These observations indicate that intracellular redox balance is significantly altered by some garlic OSC, especially DATS.

Discussion

Cancer chemoprevention by phytochemicals directed at defined molecular targets or modulated the signal transduction pathways should play an important role in reducing cancer incidence. It has been reported that *Allium* vegeta-

ble-derived OSC are able to induce the growth suppression in several tumor cell types. Using the *in vitro* model of human colon carcinoma cell lines we confirmed the antiproliferative effect of 4 OSC tested. The number of sulfur atoms in OSC including thiosulphinate allicin correlated with their potency in apoptosis induction and modulation of MMP, similarly to the induced apoptosis through oxidative modification of β-tubulin in human HCT-15 and DLD-1 colon carcinoma cell lines [20, 24]. Our data showed that order of OSC-induced cytotoxicity in Caco-2 and HT-29 cells increased in the range as follows: ALI<DAS=DADS<DATS and ALI=DAS< <DADS<DATS, respectively. Overall, both cell lines used are relatively resistant to OSC induced toxicity, because compound concentrations required to obtain significant effect are in high micromolar range. This is in agreement with recent findings [18, 19], although cytotoxic effect of lower OSC concentrations were also reported [25, 26].

ALI was less toxic than equimolar doses of other OSC tested with the exception of GSH modulation and G2/M arrest in Caco-2 cells. Small but significant G2/M arrest in HT-29 cells was induced at high concentration of ALI only.
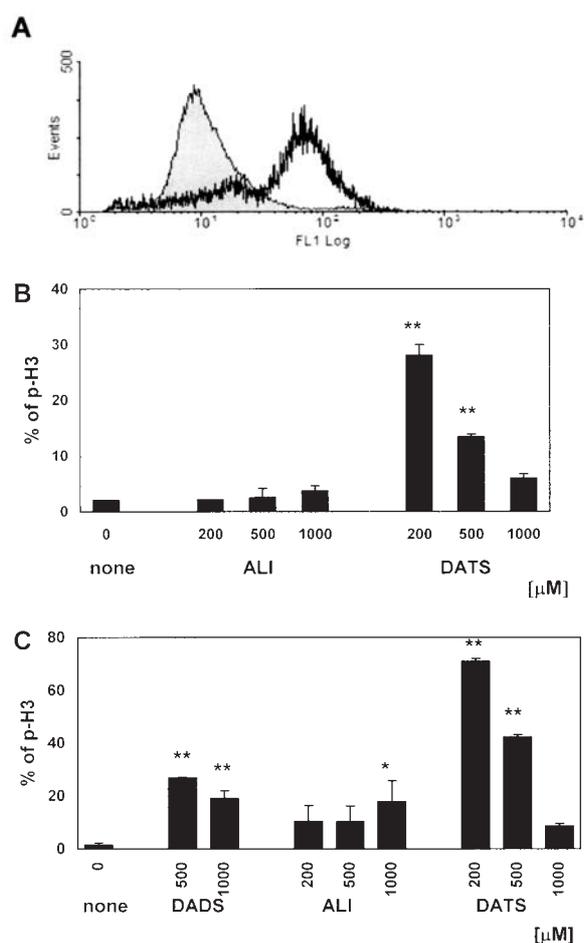

Figure 6. The effect of OSC on expression of phospho-histone H3. (A) The Caco-2 control cells (gray histogram) and cells treated with 200 μM DATS (empty histogram) for 24 h and stained with the anti-phospho-histone H3. The cells in G2/M phase of cell cycle were gated and analyzed for p-H3 positivity. (B) The Caco-2 and (C) HT-29 cells were exposed to DMSO (control) or different concentrations (200 μM, 500 μM, and 1000 μM) of OSC (DADS, ALI, and DATS) for 24 h. The cells were measured using a coulter Epics Altra flow cytometer with photomultipliers for analyzing anti-phospho-histone H3 and PI (FL1, FL2, FL4 peak and integral). Three independent experiments were performed and mean ± SE are presented. Significant difference from controls, **p<0.01.
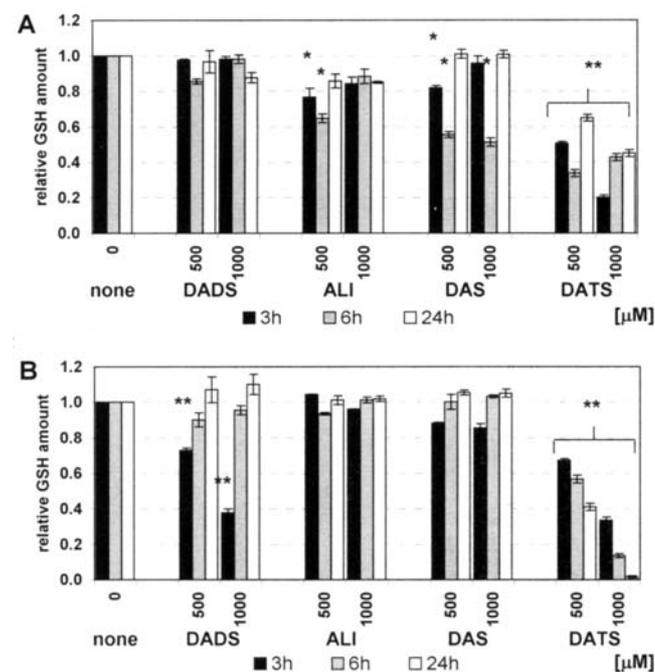

Figure 7. The effect of OSC on relative amount of intracellular reduced GSH. (A) The Caco-2 cells and (B) HT-29 cells were treated with two concentrations (500 and 1000 μM) of OSC (DADS, ALI, DAS, and DATS) for 3, 6 and 24 h. An equal volume of DMSO was added to the controls. Intracellular reduced GSH content was measured as described in "Materials and methods". Three independent experiments are shown as average of 4 replicates. The data were normalized against control and represent mean ± SD. Significant difference from controls, *p<0.05; **p<0.01.

In spite of this, increase of mitotic marker p-H3 was not observed in ALI treated Caco-2 cells. In both cell lines tested an inverse correlation of DATS concentration and p-H3 level was found. One feasible explanation is that induction of apoptosis requires the cell cycle progression from the G2/M to G1 phase as it was found recently [20]. Another possible explanation particularly in the case of DADS treatment is based on the known property of this compound. Thus, we can hypothesize that cytotoxicity is a result of combined effects of HDAC inhibition [21] and ROS production [14], the former one attenuated with increase of DADS concentration and the later one effective in the opposite direction.

There is a difference in the order of OSC effectivity in modulation of Caco-2 intracellular GSH amount (DADS<ALI<DAS<DATS) in comparison to abovementioned cytotoxic effect. The most effective compound DATS significantly decreased intracellular GSH amount that is in contrast to some published data [24, 27]. The possible reason for this discrepancy could be the high concentration range used in our study because in that study the highest level of GSH induction was found at low 25 μM concentration of DATS and decreased proportionally with increasing of DATS concentration. This is similar to our findings using higher concentrations as the GSH decrease was observed early after treatment with OSC with the exception of DATS, and no difference after 24 h of treatment was noticed in comparison to control untreated cells. Another reason for DATS induced decrease of GSH could be due to its cytotoxic effect and possible leakage of GSH out of cells. The third one could be the use of MCB assay that potentially can react in addition to GSH with protein SH groups also [28], although in our study a significant decrease of MCB fluorescence after depletion of GSH by BSO was confirmed. It was found that DADS can induce expression of MRP2 efflux pump [29], able to extrude the OSC-GSH conjugates out of cells and decrease in such a way the concentration of reduced GSH in cells. The important role of glutathione-related systems was recently confirmed in the resistance of gastric cancer cells to DADS induced apoptosis [30]. These observations are in accordance with the proposal that sulfur atoms on cysteines act as redox-sensitive "sulfhydryl switches" maintaining a physiological redox environment in the cell's interior [31].

Complex intracellular pathways are intimately linked to the effects of two promising groups of phytochemicals – OSC and isothiocyanates. In recent years, there is an emphasis on the combination therapy in which phytochemicals show a potential in combination with chemotherapeutic agents to increase the sensitivity of cancer cells to chemotherapy [32–36]. Recently some principles for the use of DADS and sulforaphane, the low affinity HDAC inhibitors [21, 37] from garlic and cruciferous vegetables in cancer treatment were proposed [38]. These representatives of OSC and isothiocyanates show similar effects as follow: chemopreventive effects shown in epidemiological studies [39–41], preferential cytotoxic effect in tumor cells in comparison to

normal cells [42, 43], induction of acute phase II enzymes [44, 45], ABC transporters [29, 46], disruption of microtubule network formation, G2/M arrest and mitotic catastrophe [20, 39, 47–50], ROS production [51, 52], and involvement of MAPK pathways [18, 46, 53] in their effects. In the present study, we demonstrate that OSC treatment especially DATS caused a significant G2/M phase cell cycle arrest in colon cancer cell lines tested. This arrest is associated with increased phosphorylation of histone H3, a marker of mitotic cells. The early effect of OSC treatment is represented by intracellular decrease of reduced GSH amount and its restoration to original level at 24 h posttreatment. The most effective compound DATS induced profound decrease of membrane mitochondrial potential and appearance of apoptotic and necrotic cells. Caco-2 cells were more sensitive to OSC treatment in comparison to HT-29 cells. Our data suggest that OSC treatment affects basic cellular pathways involving cell cycle, redox state, and mitochondrial potential. This deregulation can generate signals leading to cell apoptosis, efficiency of which is dependent on differences between OSC and cell line genetic backgrounds. Further studies are needed to clarify the useful anticarcinogenic/carcinogenic potencies of sulfur compounds and to understand the underlying mechanisms.

References

[1] AMAGASE H, PETESCH BL, MATSUURA H, KASUGA S, ITAKURA Y. Intake of garlic and its bioactive components. J Nutr 2001; 131: 955S–962S.

[2] ARIGA T, TSUJ K, SEKI T, MORITOMO T, YAMAMOTO JI. Antithrombotic and antineoplastic effects of phyto-organosulfur compounds. Biofactors 2000; 13: 251–255.

[3] GARDNER CD, MESSINA M, LAWSON LD, FARQUHAR JW. Soy, garlic, and ginkgo biloba: their potential role in cardiovascular disease prevention and treatment. Curr Atheroscler Rep 2003; 5: 468–475.

[4] KRIS-ETHERTON PM, HECKER KD, BONANOME A, COVAL SM, BINKOSKI AE et al. Bioactive compounds in foods: their role in the prevention of cardiovascular disease and cancer. Am J Med 2002; 113 Suppl 9B: 71S–88S.

[5] PARK EJ, PEZZUTO JM. Botanicals in cancer chemoprevention. Cancer Metastasis Rev 2002; 21: 231–255.

[6] MILNER JA. Garlic: its anticarcinogenic and antitumorigenic properties. Nutr Rev 1996; 54: S82–S86.

[7] HUSSAIN SP, JANNU LN, RAO AR. Chemopreventive action of garlic on methylcholanthrene-induced carcinogenesis in the uterine cervix of mice. Cancer Lett 1990; 49: 175–180.

[8] SONG K, MILNER JA. Heating garlic inhibits its ability to suppress 7, 12-dimethylbenz(a)anthracene-induced DNA adduct formation in rat mammary tissue. J Nutr 1999; 129: 657–661.

[9] GUYONNET D, BELLOIR C, SUSCHETET M, SIESS MH, LE BON AM. Liver subcellular fractions from rats treated by organo-

sulfur compounds from Allium modulate mutagen activation. Mutat Res 2000; 466: 17–26.

[10] REICKS MM, CRANKSHAW DL. Modulation of rat hepatic cytochrome P-450 activity by garlic organosulfur compounds. Nutr Cancer 1996; 25: 241–248.

[11] SCHAFFER EM, LIU JZ, MILNER JA. Garlic powder and allyl sulfur compounds enhance the ability of dietary selenite to inhibit 7,12-dimethylbenz[a]anthracene-induced mammary DNA adducts. Nutr Cancer 1997; 27: 162–168.

[12] KNOWLES LM, MILNER JA. Diallyl disulfide induces ERK phosphorylation and alters gene expression profiles in human colon tumor cells. J Nutr 2003; 133: 2901–2906.

[13] HIRSCH K, DANILENKO M, GIAT J, MIRON T, RABINKOV A et al. Effect of purified allicin, the major ingredient of freshly crushed garlic, on cancer cell proliferation. Nutr Cancer 2000; 38: 245–254.

[14] KWON KB, YOO SJ, RYU DG, YANG JY, RHO HW et al. Induction of apoptosis by diallyl disulfide through activation of caspase-3 in human leukemia HL-60 cells. Biochem Pharmacol 2002; 63: 41–47.

[15] XIAO D, CHOI S, JOHNSON DE, VOGEL VG, JOHNSON CS et al. Diallyl trisulfide-induced apoptosis in human prostate cancer cells involves c-Jun N-terminal kinase and extracellular-signal regulated kinase-mediated phosphorylation of Bcl-2. Oncogene 2004; 23: 5594–5606.

[16] WEN J, ZHANG Y, CHEN X, SHEN L, LI GC et al. Enhancement of diallyl disulfide-induced apoptosis by inhibitors of MAPKs in human HepG2 hepatoma cells. Biochem Pharmacol 2004; 68: 323–331.

[17] FILOMENI G, AQUILANO K, ROTILIO G, CIRIOLO MR. Reactive oxygen species-dependent c-Jun NH2-terminal kinase/c-Jun signaling cascade mediates neuroblastoma cell death induced by diallyl disulfide. Cancer Res 2003; 63: 5940–5949.

[18] CHEN C, PUNG D, LEONG V, HEBBAR V, SHEN G et al. Induction of detoxifying enzymes by garlic organosulfur compounds through transcription factor Nrf2: effect of chemical structure and stress signals. Free Radic Biol Med 2004; 37: 1578–1590.

[19] WU CC, CHUNG JG, TSAI SJ, YANG JH, SHEEN LY. Differential effects of allyl sulfides from garlic essential oil on cell cycle regulation in human liver tumor cells. Food Chem Toxicol 2004; 42: 1937–1947.

[20] HOSONO T, FUKAO T, OGIHARA J, ITO Y, SHIBA H et al. Diallyl trisulfide suppresses the proliferation and induces apoptosis of human colon cancer cells through oxidative modification of {beta}-tubulin. J Biol Chem 2005; 280: 41487–41493.

[21] DRUESNE N, PAGNIEZ A, MAYEUR C, THOMAS M, CHERBUY C et al. Diallyl disulfide (DADS) increases histone acetylation and p21(waf1/cip1) expression in human colon tumor cell lines. Carcinogenesis 2004; 25: 1227–1236.

[22] FERREIRA CG, EPPING M, KRUYT FA, GIACCONE G. Apoptosis: target of cancer therapy. Clin Cancer Res 2002; 8: 2024–2034.

[23] BARTKOWIAK D, HOGNER S, BAUST H, NOTHDURFT W, ROTTINGER EM. Comparative analysis of apoptosis in HL60 detected by annexin-V and fluorescein-diacetate. Cytometry 1999; 37: 191–196.

[24] WU CC, LII CK, TSAI SJ, SHEEN LY. Diallyl trisulfide modulates

cell viability and the antioxidation and detoxification systems of rat primary hepatocytes. J Nutr 2004; 134: 724–728.

[25] NAKAGAWA H, TSUTA K, KIUCHI K, SENZAKI H, TANAKA K et al. Growth inhibitory effects of diallyl disulfide on human breast cancer cell lines. Carcinogenesis 2001; 22: 891–897.

[26] HONG YS, HAM YA, CHOI JH, KIM J. Effects of allyl sulfur compounds and garlic extract on the expression of Bcl-2, Bax, and p53 in non small cell lung cancer cell lines. Exp Mol Med 2000; 32: 127–134.

[27] PINTO JT, QIAO C, XING J, RIVLIN RS, PROTOMASTRO ML et al. Effects of garlic thioallyl derivatives on growth, glutathione concentration, and polyamine formation of human prostate carcinoma cells in culture. Am J Clin Nutr 1997; 66: 398–405.

[28] MILLIS KK, LESKO SA, GAMCSIK MP. Formation, intracellular distribution and efflux of glutathione-bimane conjugates in drug-sensitive and -resistant MCF-7 cells. Cancer Chemother Pharmacol 1997; 40: 101–111.

[29] DEMEULE M, BROSSARD M, TURCOTTE S, REGINA A, JODOIN J et al. Diallyl disulfide, a chemopreventive agent in garlic, induces multidrug resistance-associated protein 2 expression. Biochem Biophys Res Commun 2004; 324: 937–945.

[30] FILOMENI G, AQUILANO K, ROTILIO G, CIRIOLO MR. Glutathione-related systems and modulation of extracellular signal-regulated kinases are involved in the resistance of AGS adenocarcinoma gastric cells to diallyl disulfide-induced apoptosis. Cancer Res 2005; 65: 11735–11742.

[31] PENNINGTON JD, WANG TJC, NGUYEN P, SUN L, BISHT K et al. Redox-sensitive signaling factors as a novel molecular targets for cancer therapy. Drug Resist Updat 2005; 8: 322–330.

[32] TAKADA Y, ANDREEFF M, AGGARWAL BB. Indole-3-carbinol suppresses NF-kappaB and IkappaBalpha kinase activation, causing inhibition of expression of NF-kappaB-regulated antiapoptotic and metastatic gene products and enhancement of apoptosis in myeloid and leukemia cells. Blood 2005; 106: 641–649.

[33] TYAGI AK, AGARWAL C, CHAN DC, AGARWAL R. Synergistic anti-cancer effects of silibinin with conventional cytotoxic agents doxorubicin, cisplatin and carboplatin against human breast carcinoma MCF-7 and MDA-MB468 cells. Oncol Rep 2004; 11: 493–499.

[34] BODO J, CHOVANCOVA J, HUNAKOVA L, SEDLAK J. Enhanced sensitivity of human ovarian carcinoma cell lines A2780 and A2780/CP to the combination of cisplatin and synthetic isothiocyanate ethyl 4-isothiocyanatobutanoate. Neoplasma 2005; 52: 510–516.

[35] POINDESSOUS V, KOEPPEL F, RAYMOND E, CVITKOVIC E, WATERS SJ et al. Enhanced antitumor activity of irofulven in combination with 5-fluorouracil and cisplatin in human colon and ovarian carcinoma cells. Int J Oncol 2003; 23: 1347–1355.

[36] KHOSHYOMN S, MANSKE GC, LEW SM, WALD SL, PENAR PL. Synergistic action of genistein and cisplatin on growth inhibition and cytotoxicity of human medulloblastoma cells. Pediatr Neurosurg 2000; 33: 123–131.

[37] MYZAK MC, KARPLUS PA, CHUNG FL, DASHWOOD RH. A novel mechanism of chemoprotection by sulforaphane: inhi-

bition of histone deacetylase. Cancer Res 2004; 64: 5767–5774.

[38] DASHWOOD RH, MYZAK MC, HO E. Dietary HDAC inhibitors: time to rethink weak ligands in cancer chemoprevention? Carcinogenesis 2006; 27(2): 344–349.

[39] MILNER JA. A historical perspective on garlic and cancer. J Nutr 2001; 131: 1027S–1031S.

[40] PAN SY, UGNAT AM, MAO Y, WEN SW, JOHNSON KC. A case-control study of diet and the risk of ovarian cancer. Cancer Epidemiol Biomarkers Prev 2004; 13: 1521–1527.

[41] GENKINGER JM, PLATZ EA, HOFFMAN SC, COMSTOCK GW, HELZLSOUER KJ. Fruit, vegetable, and antioxidant intake and all-cause, cancer, and cardiovascular disease mortality in a community-dwelling population in Washington County, Maryland. Am J Epidemiol 2004; 160: 1223–1233.

[42] SHEEN LY, LII CK, SHEU SF, MENG RH, TSAI SJ. Effect of the active principle of garlic–diallyl sulfide–on cell viability, detoxification capability and the antioxidation system of primary rat hepatocytes. Food Chem Toxicol 1996; 34: 971–978.

[43] FIMOGNARI C, BERTI F, IORI R, CANTELLI-FORTI G, HRELIA P. Micronucleus formation and induction of apoptosis by different isothiocyanates and a mixture of isothiocyanates in human lymphocyte cultures. Mutat Res 2005; 582: 1–10.

[44] GUYONNET D, BERGES R, SIESS MH, PINNERT MF, CHAGNON MC et al. Post-initiation modulating effects of allyl sulfides in rat hepatocarcinogenesis. Food Chem Toxicol 2004; 42: 1479–1485.

[45] SVEHLIKOVA V, WANG S, JAKUBIKOVA J, WILLIAMSON G, MITHEN R et al. Interactions between sulforaphane and apigenin in the induction of UGT1A1 and GSTA1 in CaCo-2 cells. Carcinogenesis 2004; 25: 1629–1637.

[46] JAKUBIKOVA J, SEDLAK J, MITHEN R, BAO Y. Role of PI3K/Akt and MEK/ERK signaling pathways in sulforaphane- and erucin-induced phase II enzymes and MRP2 transcription, G2/M arrest and cell death in Caco-2 cells. Biochem Pharmacol 2005; 69: 1543–1552.

[47] JACKSON SJ, SINGLETARY KW. Sulforaphane: a naturally occurring mammary carcinoma mitotic inhibitor, which disrupts tubulin polymerization. Carcinogenesis 2004; 25: 219–227.

[48] HERMAN-ANTOSIEWICZ A, SINGH SV. Checkpoint kinase 1 regulates diallyl trisulfide-induced mitotic arrest in human prostate cancer cells. J Biol Chem 2005; 280: 28519–28528.

[49] SMITH TK, LUND EK, PARKER ML, CLARKE RG, JOHNSON IT. Allyl-isothiocyanate causes mitotic block, loss of cell adhesion and disrupted cytoskeletal structure in HT29 cells. Carcinogenesis 2004; 25: 1409–1415.

[50] JAKUBIKOVA J, BAO Y, SEDLAK J. Isothiocyanates induce cell cycle arrest, apoptosis and mitochondrial potential depolarization in HL-60 and multidrug-resistant cell lines. Anticancer Res 2005; 25: 3375–3386.

[51] XIAO D, HERMAN-ANTOSIEWICZ A, ANTOSIEWICZ J, XIAO H, BRISSON M et al. Diallyl trisulfide-induced G(2)-M phase cell cycle arrest in human prostate cancer cells is caused by reactive oxygen species-dependent destruction and hyperphosphorylation of Cdc 25 C. Oncogene 2005; 24: 6256–6268.

[52] SINGH SV, SRIVASTAVA SK, CHOI S, LEW KL, ANTOSIEWICZ J et al. Sulforaphane-induced cell death in human prostate cancer cells is initiated by reactive oxygen species. J Biol Chem 2005; 280: 19911–19924.

[53] JAKUBIKOVA J, SEDLAK J, BACON J, GOLDSON A, BAO Y. Effects of MEK1 and PI3K inhibitors on allyl-, benzyl- and phenylethyl-isothiocyanate-induced G2/M arrest and cell death in Caco-2 cells. Int J Oncol 2005; 27: 1449–1458.